Bulletin of the Seismological Society of America, 91, 4, pp. 885–892, August 2001

MOISE: A Prototype Multiparameter Ocean-Bottom Station

by Eléonore Stutzmann, Jean-Paul Montagner, Amal Sebai, Wayne C. Crawford, Jean-Louis Thirot, Pascal Tarits, Debra Stakes, Barbara Romanowicz, Jean-Francois Karczewski, Jean-Claude Koenig, Jean Savary, Doug Neuhauser, and Steve Etchemendy

Abstract Multiple geophysical datasets were recorded during the international cooperative pilot experiment, Monterey Bay Ocean Bottom International Seismic Experiment (MOISE). This experiment, conducted from June to September 1997, demonstrated the feasibility of installing, operating, and recovering different geophysical sensors (seismometers, electromagnetometers and environmental sensors).

The seismic noise level was stable throughout the experiment. The noise level was comparable to a high noise model for periods below 15 sec and showed strong diurnal variations at longer periods. We demonstrate that these diurnal variations can be removed from the vertical component by subtracting the effect of the horizontal components, decreasing the vertical noise level by up to 40 db. We investigate possible coherence between long-period seismic, electromagnetic, and environmental data. The coherence between the vertical seismic signal and pressure and current speed is close to unity between 2×10^{-5} and 10^{-4} Hz. In particular, there is a peak of coherence at 2.3×10^{-5} Hz (12 hr), which is a consequence of tidal effects. No significant high coherence is observed with the vertical magnetic field.

The MOISE experiment demonstrates that permanent broadband seismic and geophysical observatories can now be installed on the seafloor. It also illustrates the importance of installing various kinds of geophysical sensors in order to increase the signal-to-noise ratio of seismic data, validating the concept of multiparameter ocean-bottom stations.

Introduction

The lateral resolution of tomographic models and fine-scale investigations of earthquakes or other active processes are limited by the absence of seismic stations on two-thirds of the surface of the Earth, that is, the oceanic areas. To address this problem, different workshops, such as COSOD II (1987) and ION/ODP workshop (Suyehiro *et al.,* 1995), recommended the installation of permanent oceanic seismographic stations or, even better, geophysical observatories. However, this is a very difficult task due to the hostile environmental conditions prevailing at the bottom of the ocean and the difficulty of maintaining continuous observations, retrieving data, and supplying power for long periods of time.

Several groups in France, Japan, and the United States have started preliminary experiments focused on the goal of installing permanent seafloor seismic stations. In 1992, a digital broadband seismometer was placed inside the hole 794D in the Japan sea (Suyehiro *et al.,* 1992). The same year, two sets of three-component broadband seismometers were installed for one week in the vicinity of the Mid-Atlantic Ridge (on the seafloor and in ODP hole 396b) (Montagner *et al.,* 1994a,b). In 1997, several different geophysical instruments were deployed for 3 months off of the California coast using the remotely operated vehicle (ROV) Ventana of Monterey Bay Aquarium Research Institute as part of the MOISE experiment (Stakes *et al.,* 1998). In 1998, the OSN1 borehole near Hawaii was instrumented with broadband seismometers to compare the noise level of ocean-floor and buried seismometers in the framework of the U.S. Ocean Seismic Network program (Purdy *et al.,* 1989). Collins *et al.* (1998) demonstrated that, for frequencies less than 0.1 Hz, the buried seismometer is 20–40 dB quieter than the seafloor seismometer and that the difference in noise levels is most pronounced on the horizontal components. In 1998, the first real-time ocean-bottom observatory, Hawaii-2, was installed between Hawaii and Oregon and connected to the University of Hawaii via a retired telephone cable (Butler *et al.,* 1998).

In this article, we provide a brief overview of the MOISE experiment, and we extend the preliminary results of Romanowicz *et al.* (1998) by presenting a systematic study of the seismic noise level variations. We demonstrate that the diurnal noise variations of the vertical seismic component can be removed by subtracting the effect of the horizontal components. We also investigate simultaneous recordings of seismic data, pressure, current speed, and electromagnetic signals to determine the coherence between these different parameters. High coherence between seismic and environmental data is important because it may allow us to calculate a transfer function between the parameters that can be used to increase the seismic signal-to-noise ratio (Beauduin *et al.,* 1996). In future experiments, a simultaneous inversion of seismic and electromagnetic data might help detect zones of partial melting within the crust and the lithosphere.

Description of the Experiment

The MOISE experiment took place from 17 June to 10 September 1997, in Monterey Bay, 40 km off shore of the California coast and 10 km west of the San Gregorio fault. Using a ROV (the ROV Ventana of Monterey Bay Aquarium Research Institute), the instruments were deployed on seafloor sediments at a water depth of 1015 m. In all, a three-component broadband seismometer, an electromagnetic package, a pressure gauge, a thermometer, and a current meter were installed. The seismometer was a CMG-3T and was adapted to ocean-bottom deployment by the DT/INSU. It was installed inside a cylindrical aluminum housing, partly buried inside the sediments. Its connection to the EL CHEAPO datalogger and the lithium battery package (both provided by SCRIPPS) has been performed underwater using the ROV. The datalogger and battery were in a glass Benthos sphere and could be connected to the ship via the ROV. The CTD/pressure gauge (loaned by Curt Collins) and the S4 current meter were settled with their support frame in the vicinity. Finally, the electromagnetic package, deployed nearby, was composed of magnetometers, electrometers, an internal datalogger, and a power supply (designed by UBO). Stakes *et al.* (1998) provided an overview of the experiment. The technical goal of this experiment was to demonstrate the feasibility of installing, operating, and recovering different geophysical sensors on the seafloor using a ROV.

An example of a local earthquake, a regional earthquake, and a teleseism recorded during the experiment is presented in Figure 1. The local earthquake (22 August 1997, m_b 2.9) is located 50 km from the station. The signal-to-noise ratio is high on the three components (about 9 for the *P* wave) after 1- to 5-Hz bandpass filtering. The regional earthquake (19 July 1997, m_b 5.7) occurred near the coast of Guerero in Mexico at an epicentral distance of 29°. The seismic phases can be clearly identified on the three components with a signal-to-noise ratio greater than 10 for the *P* wave. The teleseism (9 July 1997, m_b 5.9) is located near the Venezualian Coast at an epicentral distance of $\Delta = 59°$. The vertical component has a high signal-to-noise ratio (8 for the *P* wave) but on the horizontal component, only surface waves are clearly visible.

An example of five days of data recorded by the different sensors is presented in Figure 2. The seismic signal is decimated and low-pass filtered with a corner frequency of 16 mHz. The local theoretical ocean tide (Agnew, 1997) is presented for comparison at the bottom of Figure 2. Large semidiurnal amplitude variations are observed for the different signals. The coherence between the different datasets and a systematic study of the seismic noise level variations are presented in the next sections.

Coherence between the Different Datasets

To quantify the influence of current, pressure, and magnetic signals on the seismograms, we studied the coherence between these different data. The seismometer was sampled 20 times per sec. Unfortunately, the other instruments were sampled much more slowly: 1 sample per minute for the magnetometers and 1 sample per 5 minutes for the microbarometer and the current meter, making it impossible to analyze these channels in the seismic frequency band. To compare the seismic signal with the other channels, we filter and decimate the seismic signal to the sampling rate of the signal to which it is compared.

The coherence between two signals is computed using the relation:

$$\gamma^2_{S,D}(w) = \frac{|E[S^*(w) \times D(w)]|^2}{E[|S(w)|^2] \times E[|D(w)|^2]} \tag{1}$$

where $S(w)$ and $D(w)$ are the Fourier transform of the two signals. $S^*(w)$ is the complex conjugate of $S(w)$ and $E[]$ is the average ensemble for a frequency w (Bendat and Piersol, 1986). The average ensembles are computed using the multitaper spectral analysis method (Thomson, 1982, Park *et al.,* 1987 and see also Simons *et al.,* 2000 for a good description of the method). Data are windowed using functions called discrete prolate spheroidal sequences (dpss) which are solutions of an eigenvalue problem and the corresponding eigenvalues are used for weighting the windows. The ensemble averages are then estimated by averaging these weighted uncorrelated data windows.

Figure 3 presents the coherence between vertical seismic velocity and the other measured parameters for frequencies ranging from 1.1×10^{-5} Hz (1 day) to the Nyquist frequency of each channel. We used the data sequence from 26 June 1997 to 13 July 1997, that is, 17 days of continuous recording without glitches. The coherence between vertical seismic signal and both pressure and current speed is maximum and close to unity at very long period, for frequencies below 10^{-4} Hz. This high correlation is already visible on the time-series data in Figure 2. It is partly a consequence of the tide influencing all channels as can be seen at the bottom of Figure 3 where we retrieve a peak of coherence at 2.3×10^{-5} Hz (12 hr) between the seismic signal and the theoretical ocean tide. We observe no significative coherence between vertical seismic and magnetic signals.

These results show that the coherence between seismic

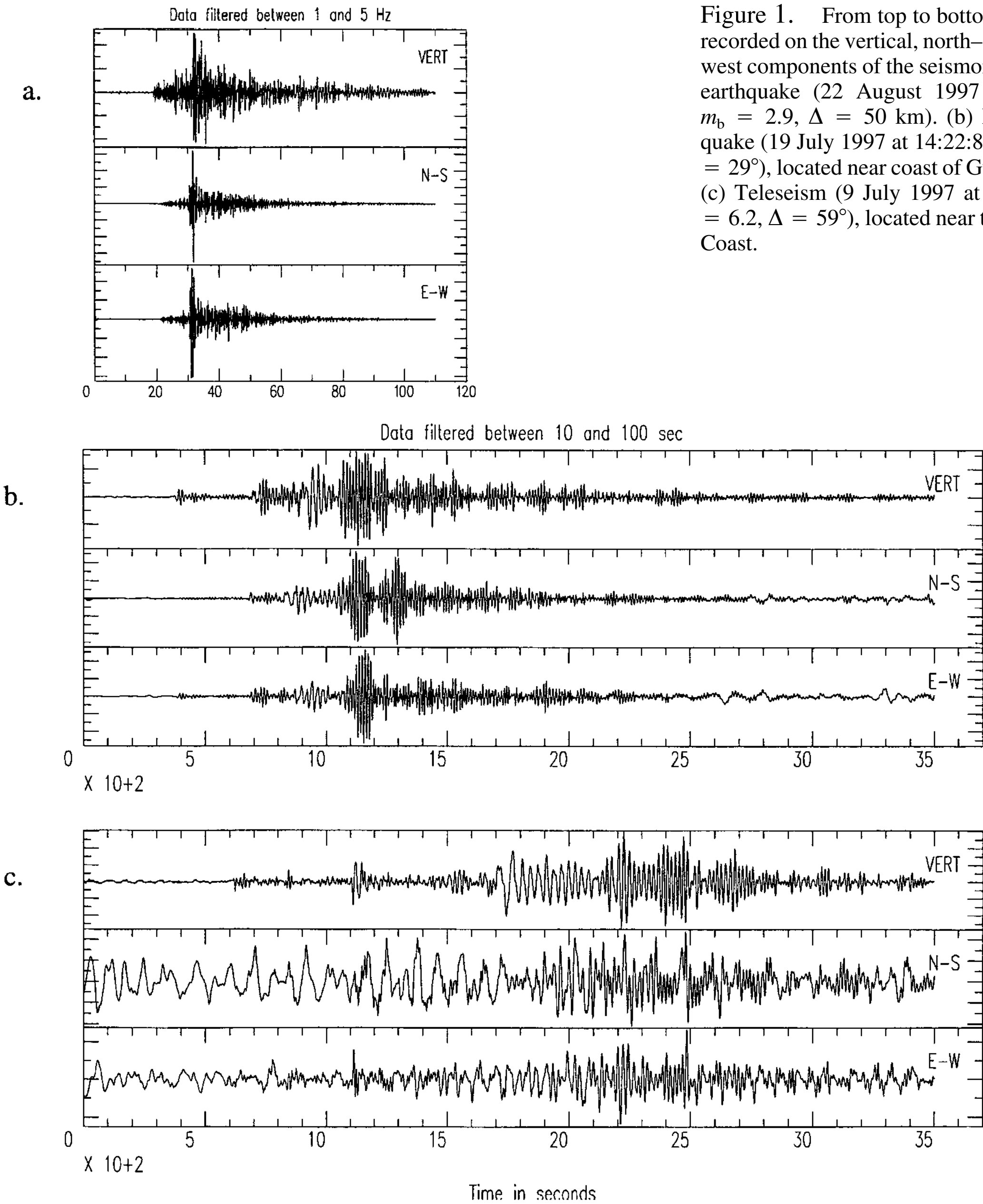

Figure 1. From top to bottom: Earthquakes recorded on the vertical, north–south, and east–west components of the seismometer. (a) Local earthquake (22 August 1997 at 13:23:59.9, $m_b = 2.9$, $\Delta = 50$ km). (b) Regional earthquake (19 July 1997 at 14:22:8.7, $m_b = 5.7$, $\Delta = 29°$), located near coast of Guerero, Mexico. (c) Teleseism (9 July 1997 at 19:24:13.1, $m_b = 6.2$, $\Delta = 59°$), located near the Venezualian Coast.

and environmental data is high at very low frequency. The coherence takes into account the phase and amplitude of the two signals. Then, a transfer function (Beauduin *et al.,* 1996) that minimizes this high coherence can be computed and applied to seismic data in order to improve the seismic signal-to-noise ratio at very low frequency. We have checked that the vertical seismic noise level can be decreased by more than 10 dB when it is corrected by using a transfer function with respect to pressure and current speed. Unfortunately, due to the low sampling rate of the environmental sensors, a similar operation could not be performed in the seismic frequency band.

To circumvent this problem, Romanowicz *et al.* (1998) studied the correlation between the amplitude of the seismic signal, expressed in terms of power spectral density, and the current velocity in the seismic band 1–100 sec. Unlike the coherence computed in this study, the correlation does not take into account the phase information and therefore cannot be used to increase the signal-to-noise ratio. However, it enables data comparison in the seismic band even when environmental data have a sampling rate of 1 sample per minute or slower. The data sets are well correlated everywhere except at periods corresponding to the microseismic peak (7–15 sec). This result is encouraging but it should be confirmed by a future experiment in which the environmental sensors have the same sampling rate as the seismic data.

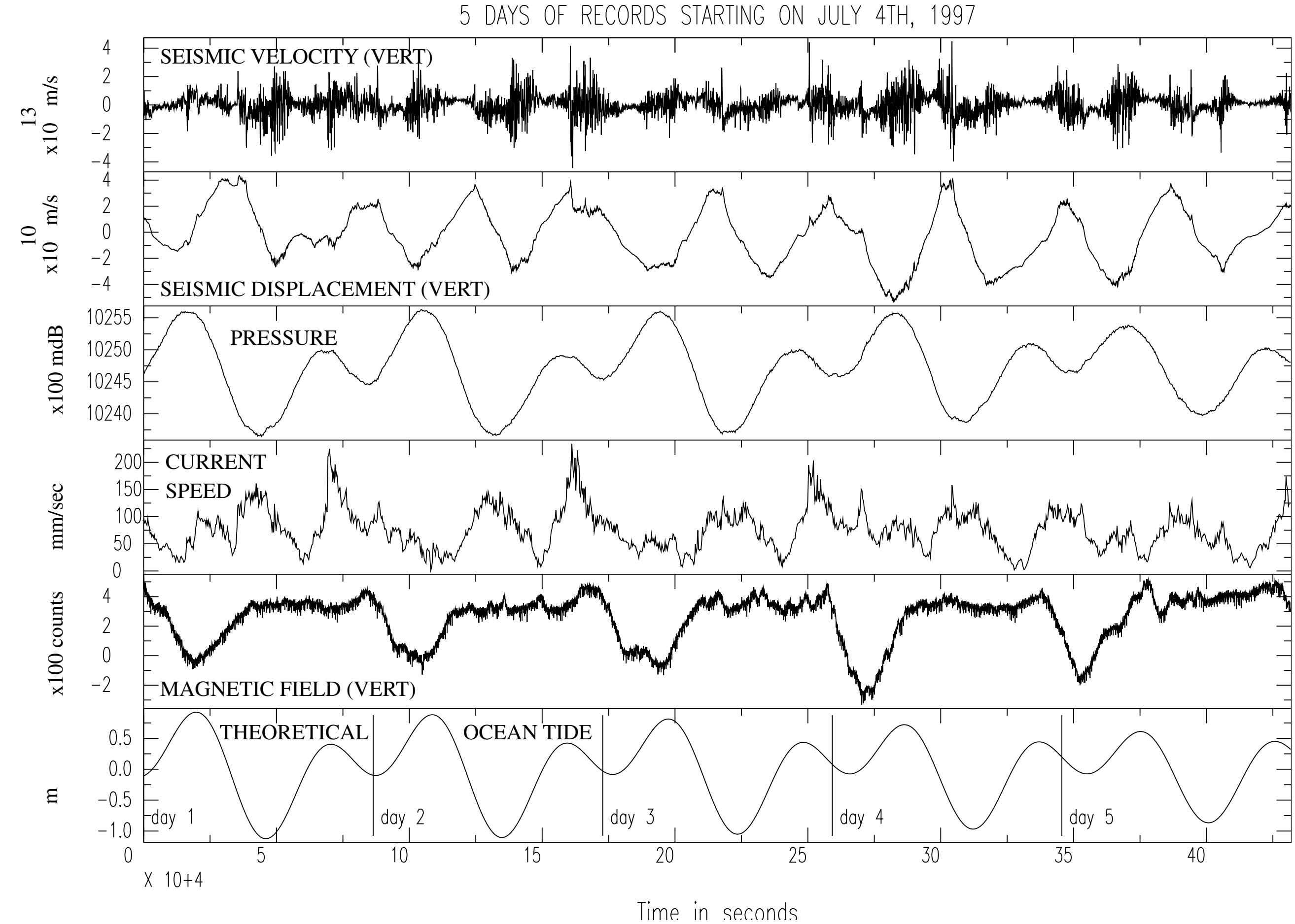

Figure 2. Five days of recording starting on 4 July 1997 at 0:00. From top to bottom: vertical seismic velocity, vertical seismic displacement, pressure, current speed, vertical magnetic field, and theoretical ocean tide.

Seismic Data Analysis

We studied the broadband seismic noise in the period range 0.2–1000 sec, computing the seismic-noise level using evenly distributed earthquake-free sequences. The power spectral density estimate averaged per week is presented in Figure 4 for the vertical and horizontal components. The dashed curves represent the high and low noise models from Peterson (1993). The noise is similar on both horizontal components and always higher than on the vertical component. Its variations from one week to another can reach 10 dB in the period range 1–10 sec for the three components. At longer period, the variations are smaller on the vertical component (15 dB) than on the horizontal component (30 dB). We observe no systematic variations of the seismic noise as a function of increasing week. For periods shorter than 1 sec, the noise is lower than the high-noise model for terrestrial stations, allowing detection of local earthquakes with amplitudes larger than 10^{-6} m/sec^2 at 1 Hz (Fig. 1). The microseismic peak is well observed on the three components between about 1 and 10 sec. For periods longer than 10 sec, the noise level is higher than the Peterson (1993) high-noise model.

The pattern of diurnal seismic-noise variations is similar on the three components (Fig. 5, left panels). The noise varies significantly for periods longer than 10 sec, increasing and decreasing four times in 24 hours, following the ocean tide. The noise is maximum when the ocean tide first derivative is minimum (Fig. 2) (Crawford and Webb, 2000). As a consequence, the signal-to-noise ratio for regional earthquakes and teleseisms, which are studied in the period range 2–100 sec, depends strongly on the hour of recording, whereas local earthquakes with most energy in the 1- to 5-Hz frequency band will have a good signal-to-noise ratio throughout the day (Fig. 1a).

The vertical seismic component is highly coherent with the north–south seismic component and less coherent with the east–west component, indicating that the vertical component was slightly tilting in the north–south direction (right, Fig. 5). Let us call θ_0 the initial tilt of the seismometer and $\varepsilon \cos(\omega t)$ the small oscillating tilt under the effect of the local currents. For period greater than about 100 sec, the

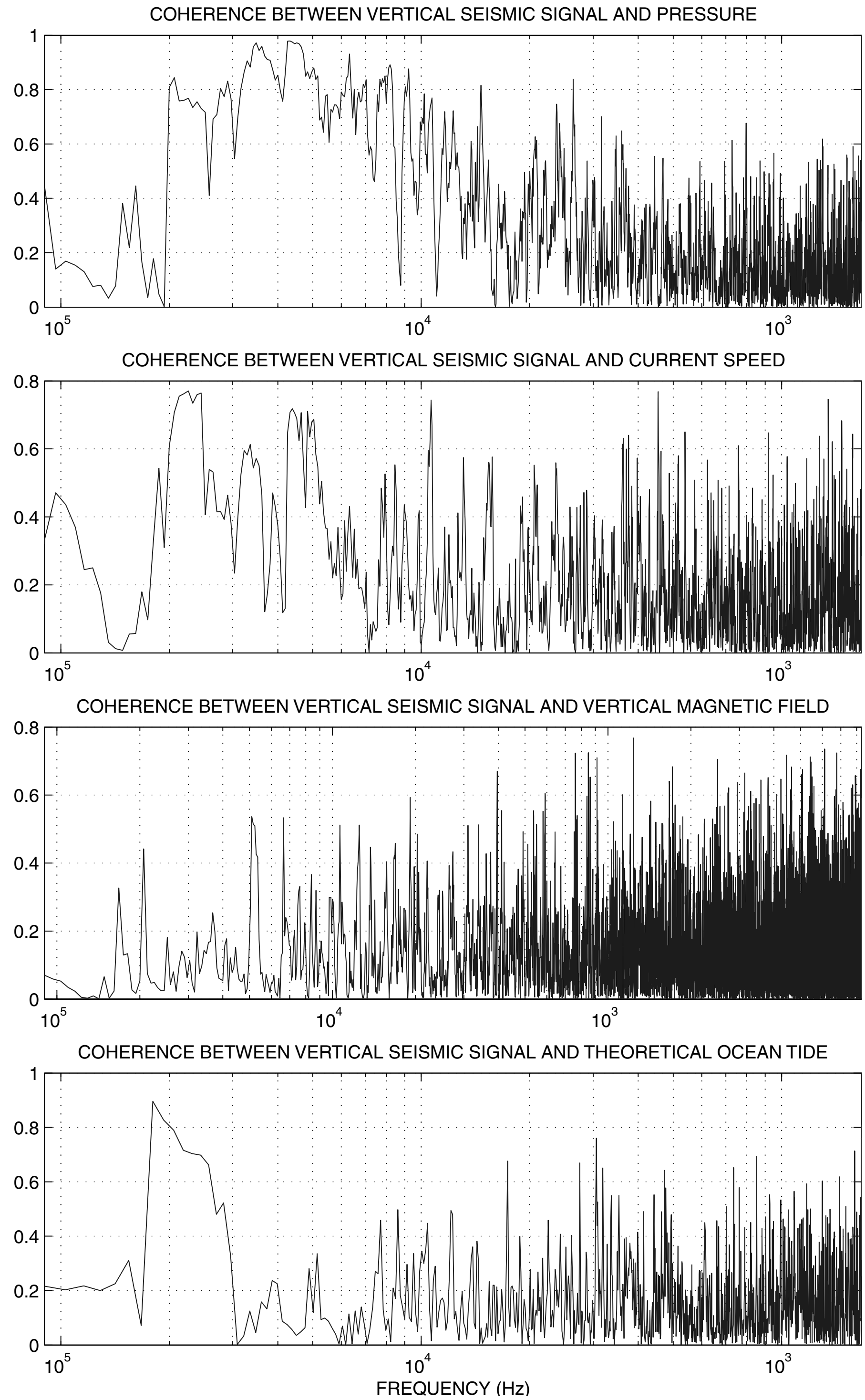

Figure 3. Coherence between vertical seismic displacement and, from top to bottom, pressure, current velocity, vertical magnetic signal, and theoretical tide as a function of frequency.

dominant effect is the change in gravitational acceleration on the seismometer due to the oscillating tilt, which can be written, respectively, for the vertical (v) and horizontal (h) accelerations, (Duennebier and Sutton, 1995; Crawford and Webb, 2000):

$$A_v = g(\cos(\theta_0 + \varepsilon \cos(\omega t)) - \cos(\theta_0))$$
$$A_h = g(\sin(\theta_0 + \varepsilon \cos(\omega t)) - \sin(\theta_0)). \quad (2)$$

When the initial tilt, θ_0 is small, we obtain

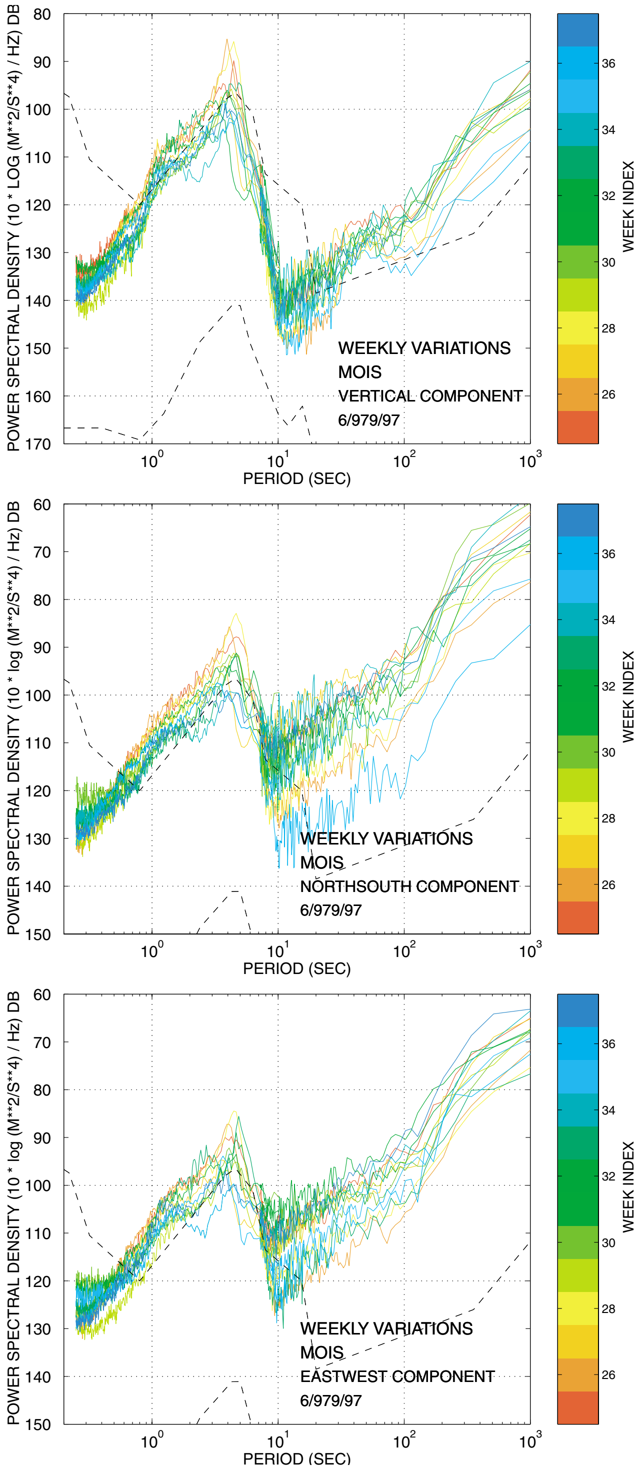

Figure 4. Weekly variations of noise power spectral density for vertical and horizontal seismograms. The color bar gives the week index. The dashed curves represent the low and high noise level of Peterson (1993).

$$A_v \propto \theta_0 A_h. \tag{3}$$

We computed the transfer functions to minimize the coherence between vertical and horizontal components by subtracting the horizontal coherent signal from the vertical signal. According to equation 3, the amplitude of the transfer function at long period gives the initial tilt of the vertical component, that is 1.4° in the north–south direction and 0.45° in the east–west direction. The vertical power spectral density after correction displays no diurnal variation, and the noise level is decreased by up to 40 dB between 10 and 50 sec (right Fig. 5).

The MOISE station was semiburied, and its noise level has been compared with three other ocean-bottom broadband stations: borehole-OSN1, seafloor-OSN1 (Collins, 1998), and buried-H2O (Butler *et al.,* 1998). For the vertical component, in the period band 0.1–10 sec, MOISE station and seafloor-OSN1 have a similar noise level, whereas borehole-OSN1 and buried-H2O are 5 to 20 dB quieter. At longer period, MOISE noise level is 10 to 30 dB higher than seafloor-OSN1, whereas buried-H2O and borehole-OSN1 are more than 30 dB less noisy. A similar pattern is observed on the horizontal components. This large noise difference can be easily explained by the strong currents along the Californian coast.

Conclusions

The MOISE experiment demonstrates that permanent broadband seismic package and auxiliary instruments can now be installed at the seafloor. We have shown that the seismic-noise level is comparable to the noise level of noisy terrestrial stations for frequencies higher than about 1 Hz. For periods greater than the microseismic peak, the noise level remains low on the vertical component down to 30 sec and increases at longer period. Seismic noise displays no systematic variations as a function of increasing week but varies throughout the day with a semidiurnal period, by 15 dB on the vertical component and by 30 dB on the horizontal components. These long-period diurnal variations can be removed on the vertical component by subtracting the effect of the horizontal components, decreasing the vertical noise level by up to 40 db.

We have investigated the simultaneous recording of seismic signal, pressure, current speed, and electromagnetic signal at very long period. The coherence between vertical seismic signal and both pressure and current speed is maximum and close to unity at very long period for frequencies between 10^{-4} Hz and 2×10^{-5} Hz. It is partly a consequence of the ocean tide influencing all channels. We observe no significant coherence between vertical seismic and magnetic signals. The observed high coherence between seismic signal and environmental parameters is important because it means that it is possible to compute a transfer function that can be applied to the seismic signal in order to

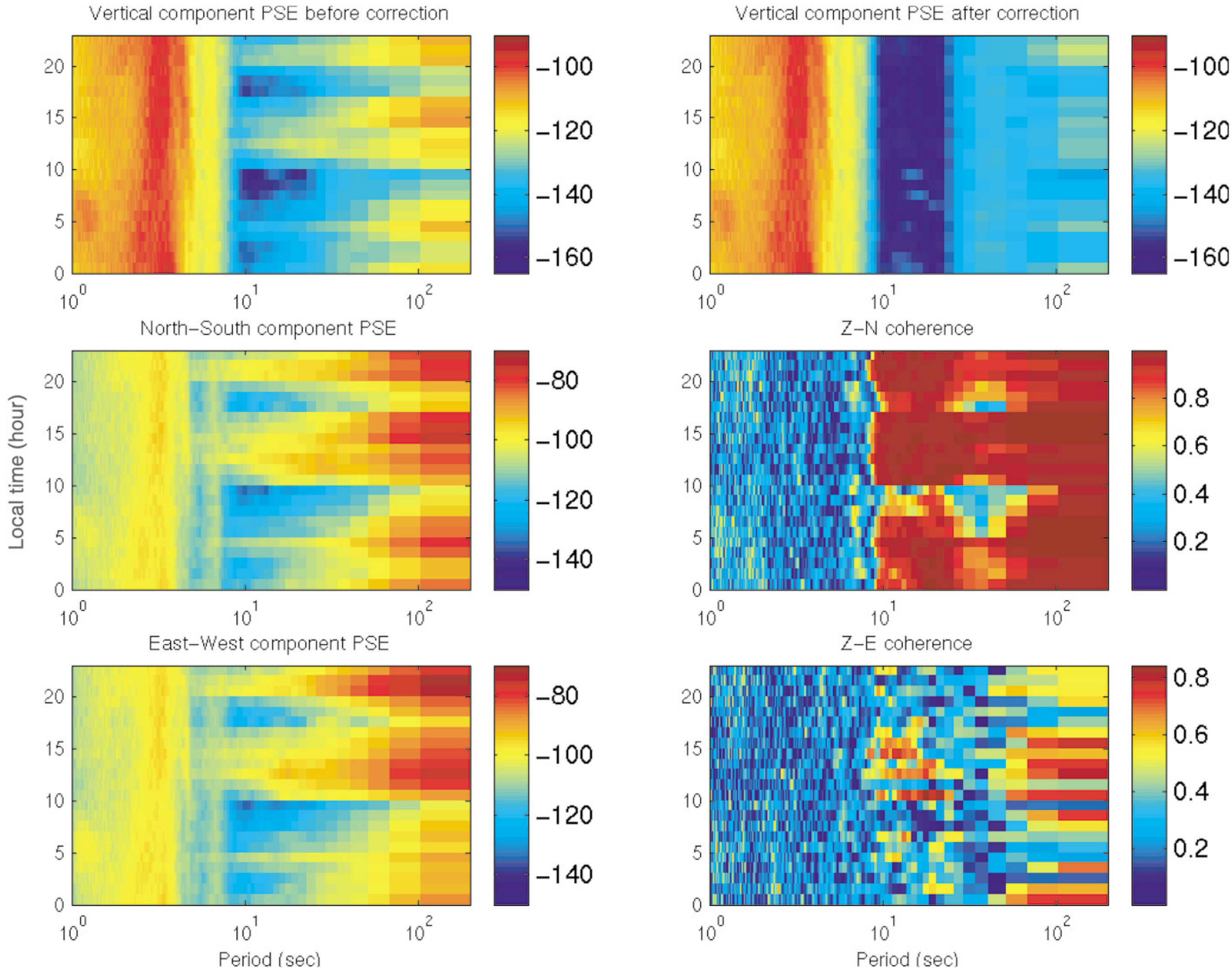

Figure 5. Left: seismic-noise power spectral density (in dB) estimated on 5 July 1997 as a function of period and local time. Top left, vertical component; middle left, north–south component; bottom left, east–west component; top right, noise power spectral density of vertical signal after correction; middle and bottom right, coherence between vertical and the north-south and east–west seismic signal, respectively.

improve the very low frequency signal-to-noise ratio by more than 10 dB.

In future ocean-bottom observatories, a higher sampling rate for electromagnetic and environmental sensors (pressure, current velocity) will facilitate a similar study in the whole seismic frequency band.

Acknowledgments

This is I.P.G.P. Contribution Number 1765 UMR CNRS 7580. This work was supported by the INSU/CNRS programme Géocéans. E. S. would like to thank F. Simons and J. Gagnepain-Beyneix for fruitful discussions, V. Ballu for computing the theoretical tide, and the two reviewers, R. Aster and F. Duennebier, for their comments.

References

Agnew, D. C. (1997). NLOADF: a program for computing ocean-tide loading, *J. Geophys. Res.* **102,** 5109–5110.

Beauduin, R., P. Lognonné, J. P. Montagner, S. Cacho, J. F. Karczewski, and M. Morand (1996). The effects of the atmospheric pressure changes on seismic signal or how to improve the quality of a station, *Bull. Seism. Soc. Am.* **86,** 1760–1769.

Butler, R., A. Chave, F. Duennebier, D. Yoerger, R. Petitt, D. Harris, F. Wooding, A. Bowen, J. Bailey, J. Jolly, E. Hobart, J. Hildebrand, and A. Dedeman (1998). Hawaii-2 observatory pioneers opportunities for remote instrumentation in ocean studies, *EOS* **81,** no. 15, 157, 162–163.

Bendat, J. S., and A. G. Piersol (1986). *Random Data: Analysis and Measurement Procedures,* Wiley-Interscience, New York.

COSODII (1987). *Rep. 2nd Conf. Sci. Ocean Drilling,* European Science Foundation, Strasbourg, France, 1987.

Collins, J., F. Vernon, J. Orcutt, and R. Stephen (1998). *Comparison of Seismographs Deployed on the Ocean Seismic Network Pilot Experiment,* Poster presented at the annual Incorporated Research Institution for Seismology (IRIS) meeting, June 1998.

Crawford, W. C., and S. C. Webb (2000). Identifying and removing tilt noise from low frequency ($<$0.1 Hz) seafloor vertical seismic data, *Bull. Seism. Soc. Am.* **90,** no. 4, 952–963.

Duennebier, F. K., and G. H. Sutton (1995). Fidelity of ocean bottom seismic observations, *Mar. Geophys. Res.* **17,** 535–555.

Dziewonski, A. M., and G. M. Purdy (1989). In *Proc. Workshop on Broad-Band Downhole Seismometers in the Deep Ocean,* Woods Hole, Massachusetts, 26–28 April 1988, Joint Oceanographic Institute and U.S. Science Advisory Committee.

Kanazawa, T., K. Suyehiro, N. Hirata, and M. Shinohara (1992). Performance of the ocean broadband downhole seismometer at site 794, In *Proc. ODP, Scientific Results, 127/128.*

Montagner, J.-P., B. Romanowicz, and J.-F. Karczewski (1994). A first step towards an oceanic geophysical observatory, *EOS Trans. Am. Geophys. Union* **75,** 150–154.

Montagner, J.-P., J.-F. Karczewski, B. Romanowicz, S. Bouaricha, P. Lognonné, G. Roult, E. Stutzmann, J. L. Thirot, D. Fouassier, J. C. Koenig (1994). The French pilot experiment OFM/SISMOBS: first scientific results on noise level and event detection, *Phys. Earth Planet. Interiors* **84,** 321–336.

Park, J., C. R. Lindberg, and D. J. Thomson (1987). Multiple taper spectral analysis of terrestrial free oscillations. Part 1, *Geophys. J. R. Astr. Soc.* **91,** 755–794.

Peterson, J. (1993). Observation and modelling of seismic background noise, *U.S. Geol. Surv. Tech. Rept. 93-322.*

Purdy, G. M., and A. M. Dziewonski (1989). In *Proc. Workshop on Broad-Band Downhole Seismometers in the Deep Ocean,* Woods Hole, Massachusetts, 26–28 April 1988, Joint Oceanographic Institute and U.S. Science Advisory Committee.

Romanowicz, B., D. Stakes, J.-P. Montagner, P. Tarits, R. Urhammer, M. Begnaud, E. Stutzmann, M. Pasyanos, J.-F. Karczewski, S. Etchemendy (1998). MOISE: A pilot experiment towards long-term seafloor geophysical observatories, *Earth Planets Space* **50,** 927–937.

Simons, F., M. Zuber, and J. Korenaga (2000). Isostatic response of the australian lithosphere: estimation of effective elastic thickness and anisotropy using multitaper spectral analysis, *J. Geophys. Res.* **105,** 19,163–19,184.

Stakes D., B. Romanowicz, J.-P. Montagner, P. Tarits, J.-F. Karczewski, S. Etchemendy, D. Neuhauser, P. McGill, J.-C. Koenig, J. Savary, M. Begnaud, M. Pasyanos (1998). MOISE: Monterrey Bay Ocean Bottom International Seismic Experiment, *EOS Trans. Am. Geophys. Union* **79,** 301–309.

Suyehiro, K., T. Kanazawa, N. Hirata, M. Shinohara, and H. Kinoshita (1992). Broadband downhole digital seismometer experiment at site 794: a technical paper, In *Proc. ODP, Scientific Results, 127/128.*

Suyehiro, K., J. P. Montagner, A. M. Dziewonski, and B. Romanowicz (1995). The international Ocean Network Structure, In *Proceedings ION/ODP International Workshop, Multidisciplinary Observatories on the Deep Seafloor, Marseille,* France, 1–3 January, 61–72.

Thomson, D. J. (1982). Spectrum estimation and harmonic analysis, *Proc. IEEE* **70,** 1055–1056.

Webb, S. C. (1998). Broadband seismology and noise under the ocean, *Rev. Geophys.* **36,** 105–142.

Institut de Physique du Globe de Paris
Department of Seismology
UMR7580, 4 Place Jussieu, 75232 Paris 05, France
(E.S., J.P.M., A.S., W.S.C., J.F.K., J.C.K., J.S.)

Université de Bretagne Occidentale
UMR6538, BP809, Brest 29285, France
(J.L.T., P.T.)

MBARI
PO Box 628
Moss Landing, California, 95039-0628
(D.S., S.E.)

UCB Seismological Laboratory
Berkeley, California
(B.R.)

DT/INSU
Saint-Maur-des-Fossés, 4 Av. de Neptune, 94, France
(D.N.)

Manuscript received 9 March 2000.